Crystal Structure Analysis of γ_1' Cu-Al-Ni Martensite Using Conventional X-Rays and Synchrotron Radiations

J. YE, M. TOKONAMI, and K. OTSUKA

The structure of the γ_1' martensite in Cu-27.14 at. pct Al-3.64 at. pct Ni alloy was analyzed by the single-crystal X-ray diffraction method using various radiations. The results confirmed that the space group of the martensite was Pnmm as Kurdjumov *et al.*[22] reported previously, and the lattice parameters were a = 4.3896(7) Å, b = 5.3424(8) Å, and c = 4.2244(7) Å. Using 3226 observed reflections collected with Mo K_α radiation, the atomic positional parameters were determined by the least-squares refinements (final discrepancy R factor being 6.36 pct), and the structure of the martensite was identified as a modified 2H one, with the stacking positions being deviated from the ideal positions. The site preferences of the Ni and Al atoms, which are off-stoichiometric from Cu_3Al, were also determined from diffraction intensities collected with various synchrotron radiations near K-absorption edges of Cu and Ni atoms.

I. INTRODUCTION

THE Cu-Al-Ni alloy is well known for the typical thermoelastic martensitic transformation[1] and associated unique mechanical behavior, such as the shape memory effect,[2-5] superelasticity,[5,6,7] and successive stress-induced martensitic transformations.[8-19] The alloy near the composition Cu-28 at. pct Al-4 at. pct Ni transforms from the β_1 parent phase to the γ_1' martensite upon cooling. The structure of the β_1 phase is of DO_3-type ordered structure.[20,21] The first step toward understanding the above behavior is to know the structure of the martensite.

The structure of the γ_1' martensite in a Cu-27.7 at. pct Al alloy was first analyzed by Kurdjumov *et al.*[22] in 1940. From X-ray rotating photographs and pole figures, they determined the orientation of one of multiple martensite variants relative to the parent phase. Then they predicted the atom positions according to the Burgers' mechanism[23] for the body-centered cubic → hexagonal close-packed (bcc → hcp) transformation and compared the prediction with an experimentally obtained rotation photograph. The space group they determined was Pnmm, and the lattice parameters were a = 4.51 Å, b = 5.20 Å, and c = 4.22 Å. The result was remarkable as an analysis without using a single crystal of the martensite. However, they did not take into account quantitative diffraction intensities in determining atom positions. Instead, they assumed idealized positions for stacking.

In 1964 and 1966, Duggin and Rachinger[21,24] studied the structure again for a Cu-28.5 at. pct Al-2.7 at. pct Ni alloy using the transformation mechanism and the X-ray Debye-Scherrer method. The lattice parameters they determined were a = 4.40 Å, b = 5.33 Å, and c = 4.24 Å, but the space group they reported was P2mm. Thus, the space groups that the two groups reported were different. One reason for the present work is to resolve this discrepancy.

Aging of the martensite at ambient temperature affects it in various ways. The most notable phenomenon is the rubberlike behavior, which is observed in the aged condition of the present alloy[25] and the Au-47.5 at. pct Cd alloy.[26] The other phenomenon is the increase of the A_s temperature after aging, which is a serious problem in the applications of shape memory alloys.[27] One possible mechanism for the aging effect, which is now being considered, is the reordering of atoms in the martensite with aging.[28] Since the atom movements, if any, associated with the reordering may be subtle, the accurate structure determination will be necessary. This determination is the second objective of the present work. Studies on the structural change with aging will be published elsewhere.

In the present alloy, the alloy composition is $Cu_{2.768}Al_{1.086}Ni_{0.146}$, which is off-stoichiometric from Cu_3Al. As known from the structure model established by Kurdjumov *et al.*,[22] there are two crystallographically unequal sites for Cu and excess Al and Ni atoms to occupy. Thus, the site occupancies of the excess Al and Ni atoms are to be determined to know the exact structure. This is the third reason for the present work.

The most standard way to determine an accurate structure is the single-crystal X-ray diffraction method. No one has attempted to use this for the present alloy, since a single crystal of the γ_1' martensite has not been available. The authors presently have a technique to make such a single crystal. The present paper reports an accurate structure analysis of the γ_1' martensite in a straightforward manner, utilizing the single-crystal X-ray diffraction method with Mo K_α radiation and with synchrotron radiations of favorable wavelengths to resolve site preference problems of off-stoichiometric Al and Ni atoms.

II. EXPERIMENTAL

A. *Specimen Preparation*

An ingot of Cu-27.14 at. pct Al-3.64 at. pct Ni alloy was prepared by melting 99.99 pct pure Cu, 99.99 pct

J. YE, Graduate Student, and M. TOKONAMI, Professor, are with the Mineralogical Institute, Faculty of Science, University of Tokyo, 7-3-1 Hongo, Bunkyo-Ku, Tokyo 113, Japan. K. OTSUKA, Professor, is with the Institute of Materials Science, University of Tsukuba, Tsukuba, Ibaraki 305, Japan.

Manuscript submitted December 4, 1989.

pure Al, and 99.9 pct pure Ni in a high-frequency vacuum induction furnace and then homogenizing at 1273 K for 86.4 ks (24 hours). The ingot, which served as raw material for growing a single crystal of the β_1 phase by a modified Bridgman method, was hot rolled into a plate 2-mm thick and cut into a suitable shape. From the grown crystal, a tensile specimen (15 × 2 × 2 mm in dimension) was spark cut. After solution treatment at 1273 K for 3.6 ks (1 hour), the specimen was quenched into ice water to retain the β_1 parent phase. The characteristic transformation temperatures were measured by observing the appearance and disappearance of surface relief of the martensitic phase during cooling and heating. They were M_s = 315.5 K, M_f = 297 K, A_s = 305 K, and A_f = 353 K.

A single crystal of the γ_1' martensite was produced by the stress-induced transformation technique reported by Otani *et al.*[29] This crystal included a small fraction of $(\bar{1}01)_{\gamma_1'}$ twins, which was introduced in the $\beta_1' \rightarrow \gamma_1'$ transformation upon unloading. Small crystals for X-ray diffraction were then separated off using an electropolishing technique with a solution of 85 pct phosphoric acid saturated with chromium trioxide. To prevent the reverse transformation by reaction heat, the electrolyte was kept at low temperatures (about 283 K) with an ice water bath. Care was taken to prevent the introduction of other martensite variants. The specimen chosen for the X-ray work was roughly spherical, with a radius of 0.15 mm.

B. *Diffraction with Mo K_α Radiation*

The preliminary X-ray diffraction work was carried out using a precession camera at ambient temperature (about 297 K) to check the quality of the crystal and to determine the space group. Figure 1 shows the typical zero layer precession photographs from which the presence of a fraction of $(\bar{1}01)$ twins was recognized (reflections deviating from the reciprocal lattice net are those diffracted by another part of the twin; one example is indicated by an arrow in Figure 1(a)). The volume ratio of the twin was estimated to be 1/5 in the later stage of X-ray work by comparing intensities of several pairs of reflections from individual parts. Those reflections, shared by two components of the twin, were excluded in the refinement process that will be described hereafter.

Intensity data for the structure analysis were collected on a Rigaku AFC-5 four-circle diffractometer equipped with graphite-monochromatized Mo K_α radiation (λ = 0.7107 Å). The integrated intensity I was obtained through ω-2θ scan, where scan width $\Delta\omega = 1.2 + 0.65 \tan\theta$ (θ is the Bragg angle for the reflection). Within the range of $2\theta < 120$ deg, 3226 reflections were collected, and 835 independent reflections were obtained after averaging symmetrically equivalent ones.

C. *Diffraction with Synchrotron Radiations*

The chemical formula of the present alloy is $Cu_{2.768}Al_{1.086}Ni_{0.146}$, while the stoichiometric one is Cu_3Al. Therefore, making clear how the excess atoms distribute in the two crystallographic sites is the key to knowing the exact structure. Usually, through X-ray crystal structure analysis, one can get only the information on the average atomic scattering factors, f_{ave}, of atom sites but not site occupancies of atoms in the sites. Occupancies of multiple atoms in a site, however, can be resolved by analyzing various sets of intensity data collected under varying atomic scattering factors of relevant atoms. From Figure 2, a diagram showing the wavelength dependence of atomic scattering factors of Cu, Ni, and Al atoms, we can see that the scattering factor of an atom is almost a constant except in the case when the wavelength is near the K-absorption edge of the atom, where the anomalous scattering effect occurs. Thus, if we use radiations with various wavelengths near the K-absorption edges of Cu and Ni atoms, we can change the scattering factors, and the site occupancies can subsequently be determined.

Following these considerations, we carried out X-ray diffraction work on the four-circle diffractometer which is set on the beam line 10A (BL-10A) in the Photon Factory (PF) of the National Laboratory for High Energy Physics, KEK, Japan. Three different wavelengths have been selected using a Si(111) monochromator to make the difference of the scattering factors between Cu and Ni atoms as large as possible. Two of them (λ_1 = 1.3850 Å and λ_2 = 1.4065 Å) are near the Cu K-absorption edge (λ_K = 1.380 Å); the other one (λ_3 = 1.4966 Å) is near the Ni K-absorption edge (λ_K = 1.488 Å); and the divergences of the three wavelengths are estimated to be less than 0.0008 Å.

The intensity measurements were carried out in an ω-2θ step-scan mode, with a step width of 0.01 deg, scan width of 1.0 deg, and scan speed of 1 s/step. The step-scan mode was employed for the careful examination of reflection profiles. Three attenuators, made of Ti, Mo, and glass, were used to protect the detector from counting too strong radiation intensities so as to assure the accuracy of counting. To monitor the decrease of source intensity with time, a standard $\bar{1}13$ reflection was measured at an interval of ten reflections. All data were normalized by this standard reflection. As a result, within the range of $2\theta < 120$ deg, 504 reflections (145 independent) were obtained for the wavelengths λ_1 and λ_2 and 373 reflections (100 independent) for λ_3.

III. RESULTS

A. *Determination of Space Group and Lattice Parameters*

Figures 1(a) through (c) show typical zero layer precession photographs in [100], [010], and [001] zone axes, respectively. From the photographs, it can be seen that (1) the three main reciprocal axes are orthogonal to each other; (2) the lattice is primitive; and (3) the diffraction patterns in Figures 1(a) through (c) have the symmetry of two-dimensional point groups 2mm, m2m, and mm2, respectively. Thus, the crystal belongs to the orthorhombic system with Laue symmetry of mmm. Paying attention to $0kl$ reflections in Figure 1(a), we note the reflections with $k + l$ = odd are systematically absent. This indicates that the crystal has an n-glide plane normal to the a^*-axis. The space group with such an n-glide plane should be one among Pnmm, $Pnm2_1$, Pnam, $Pna2_1$, Pnc2, Pncm, Pnn2, Pnnm, Pnna, and Pnnn. Apparently, the result (space group P2mm) given by Duggin

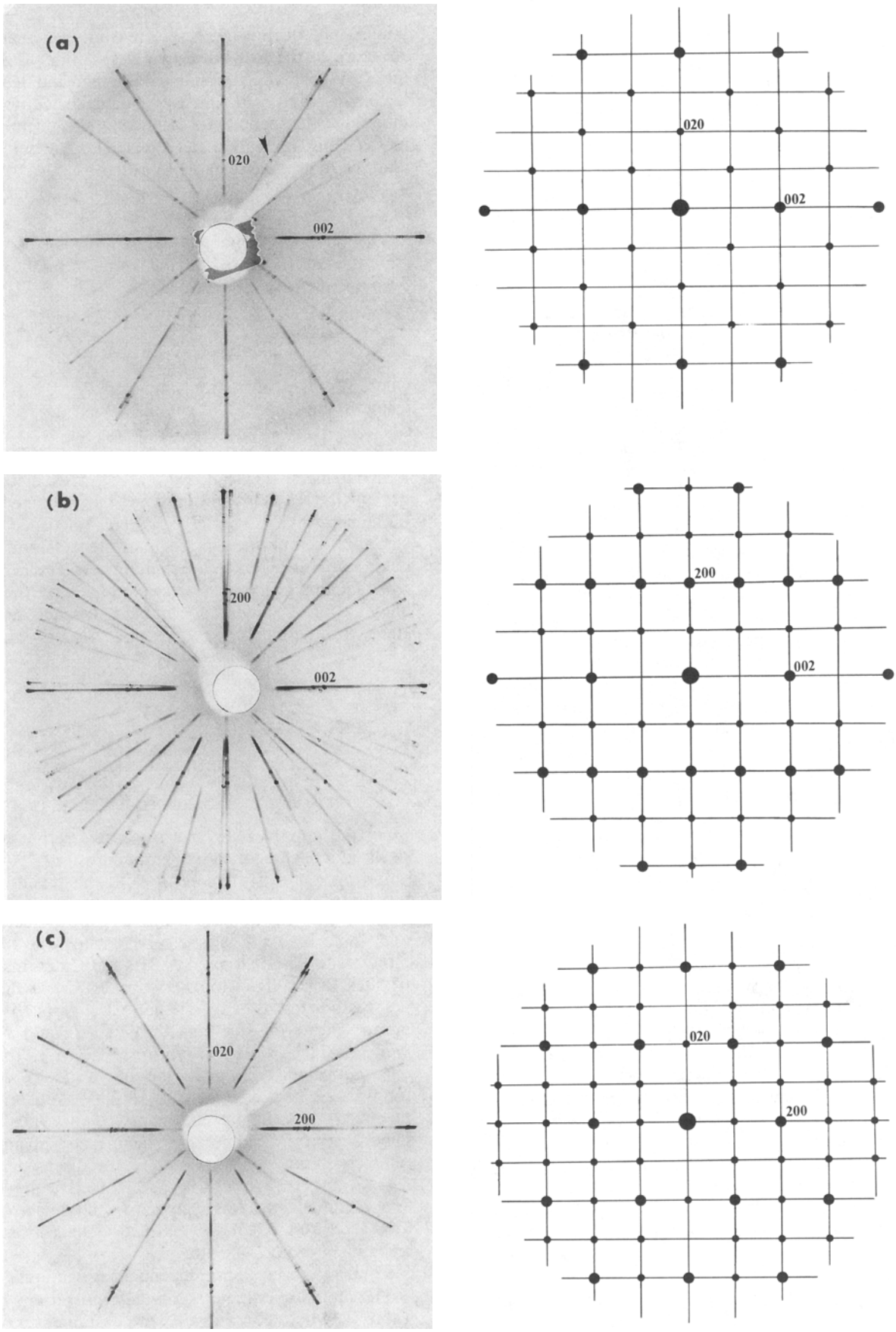

Fig. 1—Zero layer X-ray precession photographs in [100], [010], and [001] zone axes, along with the key diagrams showing (*a*) 0*kl*, (*b*) *h*0*l*, and (*c*) *hk*0 reciprocal nets, respectively. Large and small circles in the key diagrams represent strong and weak reflections, respectively.

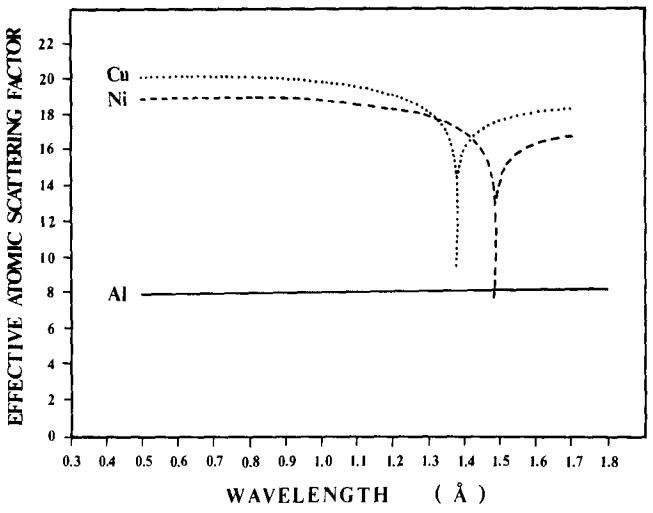

Fig. 2—Wavelength dependence of effective atomic scattering factors, f_{eff}, of Al, Ni, and Cu atoms. $f_{eff}^2 = (f_0 + f')^2 + (f'')^2$. The term f_0, the frequency-independent Thomson scattering factor for $\sin(\theta)/\lambda = 0.3$, is from *International Tables for X-ray Crystallography*;[32] f' and f'', the real and imaginary parts of the anomalous scattering factors, are from Sasaki's lists.[34]

and Rachinger[21,24] is a mistake. From $h0l$ and $hk0$ reflections in Figures 1(b) and (c), we observe that the reflections are all present. This fact excludes the presence of any *a*-, *c*-, or *n*-glide plane normal to the b^*- or c^*-axis. Thus, only two space groups, Pnmm and $Pnm2_1$, remain possible among them. The distinction between the two lies in whether the center of symmetry is present or not. Here, we assumed that the crystal has the center of symmetry and then carried out structural analyses. As will be described in the next section, the result was quite consistent with that assumption. Therefore, we conclude that the space group is Pnmm. This result agrees with that reported by Kurdjumov *et al.*[22]

The lattice parameters have been determined by the least-squares method using 25 reflections obtained from the four-circle diffractometer. The results are shown in Table I.

B. *Structure Analysis*

There are three kinds of parameters to be determined in this stage: (1) *x*, *y*, and *z* positional parameters of atomic sites, (2) temperature factors of atoms, and (3) site occupancies of atoms. As described in the previous sections, the alloy is off-stoichiometric, and the excess Al and Ni atoms distribute in two crystallographic sites. In order to resolve such a site occupancy problem, we used various synchrotron radiations to collect diffraction intensity data. However, since the wavelengths λ_1, λ_2, and λ_3 near the *K*-absorption edges of Cu and Ni atoms are roughly 2 times longer than that of Mo K_α radiation, the spatial resolution of the analysis using such a long wavelength will decline. For this reason, we analyzed the structure in the following two steps: first, to determine the *x*, *y*, and *z* positional parameters and temperature factors of atoms using intensity data collected with Mo K_α radiation and second, to determine site occupancies of atoms using intensity data collected with synchrotron radiations of wavelengths λ_1, λ_2, and λ_3.

Table I. Lattice Parameters for γ_1' Cu-Al-Ni Martensite

a (Å)	*b* (Å)	*c* (Å)
4.3896(7)	5.3424(8)	4.2244(7)

1. *Structure analysis using intensity data collected with Mo K_α radiation*

The observed structure factors $|F(\text{obs})|$ used for the structure analysis are derived from the following diffraction intensity formula:

$$I = K \frac{1 + \cos^2 2\theta_M \cdot \cos^2 2\theta}{\sin^2 2\theta (1 + \cos^2 2\theta_M)} |F(\text{obs})|^2$$

where I is the diffraction intensity; θ_M, the monochromator Bragg angle; $(1 + \cos^2 2\theta_M \cdot \cos^2 2\theta)/\sin^2 2\theta(1 + \cos^2 2\theta_M)$, the Lorentz polarization factor; and K, the scale factor. After absorption corrections for a spherical crystal shape ($\mu R = 4.7$), the structure analysis was carried out using the standard least-squares method (program LINUS[30]) by minimizing the weighted sum of differences of observed (F(obs)) and calculated (F(calc)) structure factors (the reciprocal of the square of standard deviation was taken as the weight, w). The accuracy of least-squares refinements was evaluated by the discrepancy factor, R, and the weighted residual factor, wR. Here, R is defined by

$$R = \frac{\Sigma \| F(\text{obs})| - |F(\text{calc}) \|}{\Sigma |F(\text{obs})|}$$

and wR by

$$wR = \frac{\Sigma w(|F(\text{obs})| - |F(\text{calc})|)^2}{\Sigma w |F(\text{obs})|^2}$$

For the initial value of least-squares refinements, the idealized model reported by Kurdjumov *et al.*[22] was used. Referring to the structures of both the parent phase[31] and the β_1'' martensite phase,[12] we assumed the distributions of atoms in basal planes as follows (see Figure 3 and Table II(a)): Al atoms fully occupy site I; extra Al atoms, site II; Ni atoms, site III; and Cu atoms, the rest of sites II and III. Atoms occupying sites I through III are symbolized as Al, Cu1, and Cu2, respectively. The atomic scattering factors for Cu, Al, and Ni atoms were taken from *International Tables for X-ray Crystallography*.[32] For Kurdjumov's model, the R factor was 29.85 pct (wR = 30.18 pct). Apparently, this idealized model is not reasonable. By varying the scale factor, isotropic temperature factor, and positional parameters iteratively, we obtained the discrepancy factor R = 7.40 pct (wR = 7.05 pct). Finally, the isotropic temperature factor was changed to the anisotropic one, together with the isotropic extinction correction, and the refinement converged to give R = 6.36 pct (wR = 5.87 pct) with all 835 independent reflections.

The atomic parameters thus determined are shown in Table II, where coordinates were described in two ways according to different origin choices. Table III shows the calculated structure factors, F(calc), and observed structure factors, F(obs). Due to size limitations, only a part

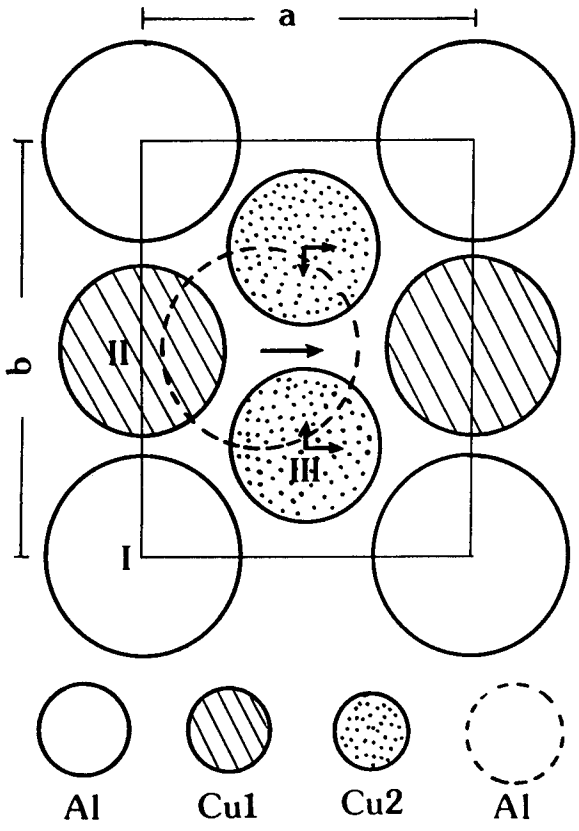

Fig. 3—Crystal structure of γ_1' Cu-Al-Ni martensite described in the conventional way. Dotted circle represents the Al atom in the second layer. Arrows indicate the relative atom displacements to the Al atoms in the first layer from the ideal 2H positions.

of the data for the 835 reflections is given. Good agreement between calculated and observed structure factors can be seen in the table.

2. *Structure analysis using intensity data collected with synchrotron radiations*

In the last section, we determined positional parameters of atoms, but site preference problems for excess Al and Ni atoms still remain because the problem is impossible to solve by using one-wavelength X-ray diffraction method. From Figure 4, a diagram showing the relationship between average atomic scattering factors, f_{ave}, and atomic occupancy parameters of site II, it may be seen that any definite value of f_{ave} is represented by a contour line (broken line in the figure) but not a point. In other words, those site occupancies of atoms distributed along the broken line have the same f_{ave} value. Therefore, even if the f_{ave} value of the site has been determined, we still cannot conclude a definite site occupancy. However, if we use various wavelengths λ_1, λ_2, and λ_3, the situation will become different. Since λ_1, λ_2, and λ_3 are radiations with wavelengths near the *K*-absorption edges of Cu and Ni atoms, contour lines of f_{ave} in Figures 4(a) through (c) behave totally differently. Thus, if we determine average scattering factors, f_{ave}, of the site under different wavelength conditions, we can determine, in principle, site occupancy parameters for the site by comparing these contours. In the present work, considering the accuracy of collected intensities and the amounts of excess Al and Ni atoms, instead of determining average atomic scattering factors, f_{ave}, directly, we assumed chemical compositions for the sites and then

Table II. Atomic Parameters and Anisotropic Temperature Factors for γ_1' Cu-Al-Ni Martensite

(a) Atomic Parameters

	Wyckoff Notation	Atom	*x*	*y*	*z*
Origin at $\bar{1}$[33]	2(a)	Al	5/6 − 0.0163(5)	1/4	1/4
	2(b)	Cu1	5/6 − 0.0160(1)	3/4	1/4
	4(f)	Cu2	1/3 − 0.0146(1)	1/2 + 0.00056(8)	1/4
Conventional Coordinates					
Origin at 1/6, −1/4, −1/4 from the center of symmetry		Al	0 − 0.0163(5)	0	0
			1/3 + 0.0163(5)	1/2	1/2
		Cu1	0 − 0.0160(2)	1/2	0
			1/3 + 0.0160(2)	0	1/2
		Cu2	1/2 − 0.0146(1)	1/4 + 0.00056(8)	0
			1/2 − 0.0146(1)	3/4 − 0.00056(8)	0
			5/6 + 0.0146(1)	1/4 − 0.00056(8)	1/2
			5/6 + 0.0146(1)	3/4 + 0.00056(8)	1/2

Atom Distributions Assumed for Least-Squares Refinements

Site	I	II	III
Symbol	Al	Cu1	Cu2
Composition	Al	$Cu_{0.914}Al_{0.086}$	$Cu_{0.927}Ni_{0.073}$

(b) Anisotropic Temperature Factors

Atom	β_{11}	β_{22}	β_{33}	β_{12}	β_{13}	β_{23}	β_{eq}**
Al	0.0128	0.0097	0.0113	0	0	0	0.97
Cu1	0.0119	0.0076	0.0112	0	0	0	0.86
Cu2	0.0117	0.0073	0.0107	0.00002	0	0	0.74

*Anisotropic temperature factors are expressed in the form of exp $[-(\beta_{11}h^2 + \beta_{22}k^2 + \beta_{33}l^2 + 2\beta_{12}hk + 2\beta_{13}hl + 2\beta_{23}kl)]$.
**β_{eq} is equivalent isotropic value.

Table III. Observed and Calculated Structure Factors

h	k	l	F(obs)	F(calc)
0	1	1	28.91	28.31
0	3	1	20.59	19.99
0	5	1	14.36	14.11
0	7	1	8.51	7.93
0	9	1	6.88	6.52
0	11	1	3.87	3.58
0	0	2	142.38	143.09
0	2	2	24.93	24.65
0	6	2	10.66	11.84
0	8	2	36.27	35.47
0	10	2	4.90	5.90
0	12	2	14.70	14.14
0	1	3	17.73	17.84
0	3	3	13.76	13.63
0	5	3	11.43	10.88
0	7	3	6.36	6.72
0	9	3	5.41	5.71
0	11	3	3.18	3.20
0	2	4	13.67	14.73
0	4	4	59.28	58.39
0	6	4	9.20	9.15
0	8	4	28.40	27.86
0	10	4	4.30	5.02
0	1	5	9.63	9.93
0	3	5	7.82	8.35
0	5	5	7.22	7.52
0	7	5	4.64	5.06
0	9	5	4.73	4.49
0	11	5	2.06	2.56
0	0	6	46.09	45.21
0	2	6	8.42	9.07
0	4	6	35.84	35.41
0	6	6	5.59	6.60
0	8	6	20.38	19.82
0	10	6	3.18	3.88
0	1	7	6.27	6.04
0	3	7	5.16	5.32
0	5	7	5.41	5.04
0	7	7	3.27	3.57
0	9	7	3.61	3.21
0	0	8	26.59	25.54
0	2	8	5.93	5.90
0	4	8	22.28	21.29
0	6	8	3.95	4.56
0	8	8	13.84	13.04
0	1	9	4.38	3.77
0	3	9	3.61	3.37
0	5	9	3.78	3.22
0	0	10	15.04	14.55
0	2	10	4.04	3.74
1	0	0	12.94	14.79
1	1	0	25.31	25.23
1	2	0	63.97	61.14
1	3	0	21.71	19.70
1	4	0	8.51	8.61
1	5	0	12.81	11.36
1	6	0	26.52	25.71
1	7	0	9.03	8.56
1	8	0	3.95	3.78
1	9	0	5.33	4.86
1	10	0	10.06	9.83
1	11	0	4.13	4.11

Table III. Cont. Observed and Calculated Structure Factors

h	k	l	F(obs)	F(calc)
1	12	0	2.15	1.81
1	0	1	25.86	29.01
1	1	1	9.98	10.74
1	2	1	127.61	126.31
1	3	1	8.34	8.42
1	4	1	16.09	17.08
1	5	1	4.13	4.95
1	6	1	54.47	54.64
1	7	1	3.61	3.77
1	8	1	7.22	7.76
1	9	1	3.01	2.16
1	10	1	22.54	21.17
1	11	1	2.58	1.83
1	12	1	2.58	3.77
1	0	2	10.67	11.68
1	1	2	18.09	19.76
1	3	2	16.69	16.01
1	4	2	12.21	7.29
1	5	2	10.06	9.89
1	6	2	22.80	22.78
1	7	2	7.99	7.82
1	8	2	8.25	3.51
1	9	2	4.81	4.54
1	10	2	9.37	9.16
1	11	2	4.13	3.88
1	12	2	3.70	1.72
1	0	3	18.59	18.55
1	1	3	6.27	6.84
1	2	3	88.08	86.20
1	3	3	5.59	5.84
1	4	3	12.81	12.72
1	5	3	3.87	3.85
1	6	3	45.65	43.47
1	7	3	3.44	3.19
1	8	3	5.76	6.79
1	9	3	2.32	1.90
1	10	3	19.69	18.48
1	11	3	2.15	1.63
1	12	3	2.92	3.41
1	0	4	6.45	6.73
1	1	4	11.35	11.33
1	2	4	27.66	30.19
1	3	4	9.54	10.18
1	4	4	4.73	5.03
1	5	4	7.31	7.15
1	6	4	17.37	16.76
1	7	4	6.27	6.19
1	8	4	2.84	2.90
1	9	4	3.70	3.79
1	10	4	7.91	7.56
1	11	4	3.52	3.28
1	0	5	10.40	10.65
1	1	5	3.87	3.88
1	2	5	46.85	49.94
1	3	5	3.44	3.62
1	4	5	8.42	8.58
1	5	5	2.66	2.69
1	6	5	31.08	30.13
1	7	5	2.58	2.40
1	8	5	4.56	5.37
1	9	5	1.72	1.50
1	10	5	14.79	14.42

Table III. Cont. Observed and Calculated Structure Factors

h	k	l	F(obs)	F(calc)
1	11	5	1.29	1.30
1	0	6	3.78	4.03
1	1	6	6.79	6.69
1	2	6	16.60	17.24
1	3	6	6.27	6.39
1	4	6	3.27	3.38
1	5	6	5.16	4.92
1	6	6	11.60	11.11
1	7	6	4.21	4.50
1	8	6	1.72	2.20
1	9	6	2.92	2.85
1	10	6	5.67	5.61
1	0	7	6.27	6.73
1	1	7	2.32	2.39
1	2	7	28.32	28.60
1	3	7	2.58	2.31
1	4	7	5.67	5.82
1	5	7	1.98	1.82
1	6	7	20.30	19.48
1	7	7	0.69	1.68
1	8	7	3.44	3.92
1	9	7	0.69	1.08
1	0	8	2.84	2.59
1	1	8	4.13	4.20
1	2	8	10.23	9.93
1	3	8	3.95	4.10
1	4	8	2.41	2.27
1	5	8	3.61	3.27
1	6	8	7.22	7.04
1	7	8	3.61	3.04
1	8	8	1.46	1.54
1	0	9	3.95	4.36
1	1	9	0.69	1.49
1	2	9	17.45	16.58
1	3	9	1.03	1.46
1	4	9	3.52	3.85
1	5	9	0.60	1.17
1	6	9	12.46	12.04
1	0	10	1.46	1.64
1	1	10	2.92	2.56
1	2	10	6.45	5.73
2	0	0	91.64	94.80
2	1	0	16.63	17.91
2	2	0	15.66	15.49
2	3	0	12.47	12.93
2	4	0	59.58	58.02
2	5	0	9.03	9.58
2	6	0	6.96	7.39
2	7	0	5.59	5.58
2	8	0	24.26	23.23
2	9	0	4.64	4.64
2	10	0	3.27	3.71
2	11	0	2.23	2.57
2	12	0	9.28	9.23
2	1	1	15.41	14.84
2	2	1	19.46	18.43
2	3	1	12.12	10.84
2	4	1	66.42	64.24
2	5	1	8.42	8.17
2	6	1	10.14	9.02
2	7	1	5.50	4.81
2	8	1	26.59	26.19

Table III. Cont. Observed and Calculated Structure Factors

h	k	l	F(obs)	F(calc)
2	9	1	4.13	4.02
2	10	1	4.21	4.49
2	11	1	2.15	2.24
2	12	1	10.40	10.50
2	1	2	12.39	14.25
2	2	2	11.70	12.60
2	3	2	10.23	10.75
2	4	2	48.32	49.87
2	5	2	8.68	8.44
2	6	2	6.27	6.71
2	7	2	5.16	5.15
2	8	2	22.02	21.37
2	9	2	4.64	4.34
2	10	2	3.44	3.51
2	11	2	2.15	2.43
2	12	2	9.11	8.70
2	1	3	9.54	9.91
2	2	3	14.10	12.87
2	3	3	7.99	7.81
2	4	3	48.17	48.47
2	5	3	6.10	6.48
2	6	3	11.43	7.53
2	7	3	4.73	4.11
2	8	3	22.19	22.30
2	9	3	3.52	3.55
2	10	3	6.96	4.03
2	11	3	2.15	2.00
2	12	3	9.54	9.35
2	0	4	50.08	47.17
2	1	4	7.82	8.69
2	2	4	7.39	8.11
2	3	4	6.62	7.15
2	4	4	36.28	34.15
2	5	4	5.93	6.24
2	6	4	4.81	5.31
2	7	4	3.87	4.13
2	8	4	16.85	16.95
2	9	4	3.52	3.61
2	10	4	2.58	3.00
2	11	4	1.72	2.06
2	0	5	37.62	41.04
2	1	5	5.84	5.94
2	2	5	7.39	8.12
2	3	5	4.73	5.05
2	4	5	31.61	31.39
2	5	5	4.90	4.60
2	6	5	4.98	5.69
2	7	5	2.92	3.15
2	8	5	17.03	16.71
2	9	5	3.35	2.81
2	10	5	2.49	3.27
2	11	5	1.55	1.61
2	0	6	27.11	27.01
2	1	6	5.07	5.33
2	2	6	4.90	5.26
2	3	6	4.90	4.63
2	4	6	21.76	21.42
2	5	6	4.64	4.33
2	6	6	3.27	3.92
2	7	6	3.27	3.03
2	8	6	12.38	12.16
2	9	6	2.92	2.72

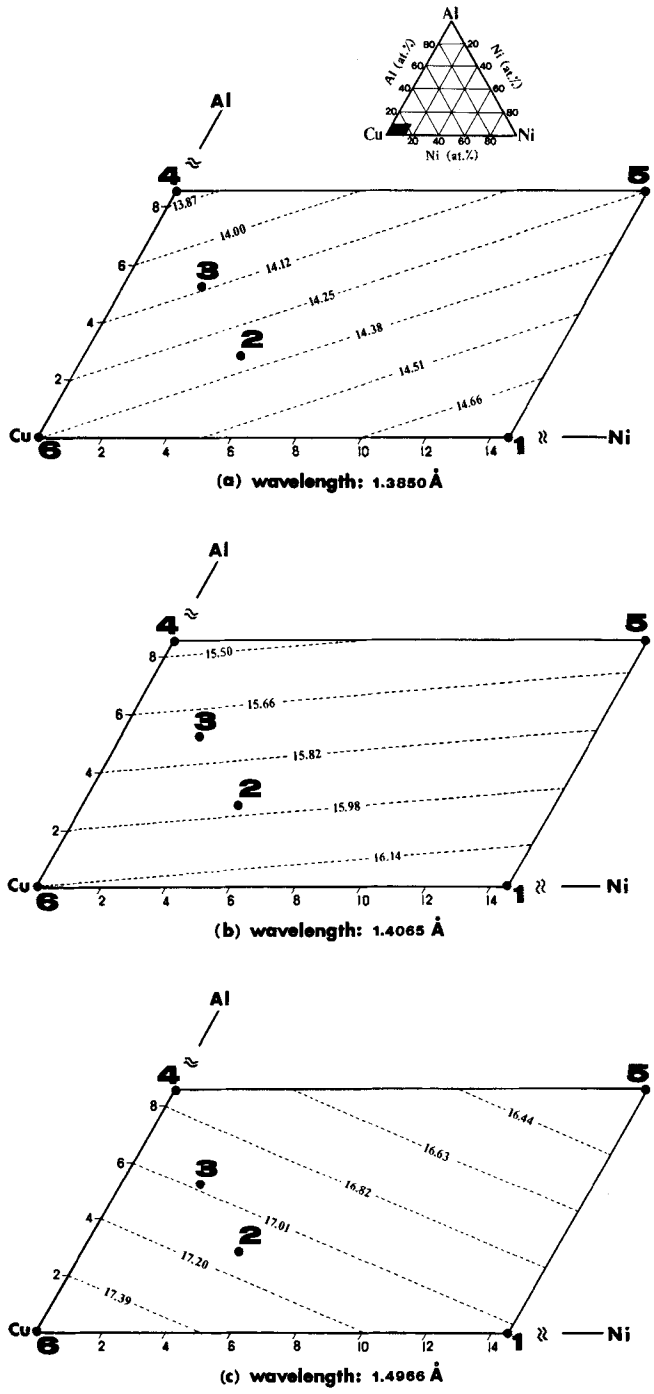

Fig. 4—A part of the Cu-Al-Ni triangular composition diagram (solid part) showing the relationships between calculated average atomic scattering factors, f_{ave}, and atom occupancy parameters in site II. (*a*) for λ_1, (*b*) for λ_2, and (*c*) for λ_3. Solid circles indicate the compositions of atom distribution models used for the least-squares. See Section III–B–2 for a detailed explanation of this figure.

made least-squares refinements to see the consistency of the model with experimental data. The model which has the smallest R factor may be regarded as the reliable one.

The least-squares refinements were carried out using program LINUS[30] for three sets of intensity data collected with wavelengths λ_1, λ_2, and λ_3, of which the observed structure factors, F(obs), were deducted from the following equation:

$$|F(\text{obs})|^2 = K_a \cdot K_s \cdot K_l \cdot I$$

where K_a is the attenuator factor; K_s is the scale factor which is corrected by the intensities of the standard reflection $\bar{1}13$; K_l is the reciprocal of the Lorentz factor; and I is the integrated intensity obtained by summing up the counts of all 101 scan steps after subtracting backgrounds. The polarization factor was assigned unity because the incident X-ray was horizontally polarized. Anomalous scattering factors were taken from the list of Sasaki[34] that was calculated using the corrected version[35] of the method presented by Cromer and Liberman.[36]

For least-squares refinements, six typical atom distribution models, whose compositions are listed in Table IV and plotted in Figure 4, were assumed. The results are shown in Figure 5. It may be seen that the discrepancy factor, R, of least-squares depends upon the model employed. The minimum value, $R = 5.1$, was obtained for model 4, for which extra Al occupy site II and Ni occupy site III. It is interesting to note that the least-squares refinements, using three sets of reflections collected with radiations of different wavelengths near the Cu K-absorption edge and Ni K-absorption edge, have given the minimum R factor for the same model. Therefore, model 4 is believed to be the most reliable combination of atoms.

Comparing the site occupancies of off-stoichiometric Al and Ni atoms in the γ_1' martensite phase determined above with those in the β_1 parent phase,[31] we find that the site occupancies in both phases are just the same. This fact is consistent with the diffusionless nature of the present transformation.

IV. DISCUSSION

The structure of the γ_1' martensite is shown in Figure 3, where the second layer is represented by the Al atom (dotted one) for the centrosymmetrical relation of the two basal layers. Because the basal plane is a close-packed one, it may be expected that the second layer sits at the center of the triangular atom configuration, *i.e.*, the $a/3$ position, as reported by Kurdjumov *et al.*[22] However, the results of least-squares refinements in Table II(a) clearly show that there were considerable atom displacements from the ideal positions. In the table, the fractional numbers represent the ideal positions, and the decimal numbers, the deviations from the ideal positions. We find that the atom displacements occur not only along the a-axis but also along the b-axis; the amounts of displacements along the a-axis are different from each other, the smallest one being associated with atom Cu2. The displacements are also illustrated in Figure 3 by arrows, which represent the direction and magnitude of atom displacements relative to the Al atoms of the first layer. It can be seen that atoms in the second layer (illustrated with dotted circle) are displaced from the $a/3$ ideal positions considerably, and Cu2 atoms in the first layer are also displaced from the original symmetric positions. This is the first observation even among β-phase alloys.

To account for the above atom displacements, the rigid sphere model, which Tadaki *et al.* used to explain the atom displacements in Cu-Zn martensite,[37] may also be appropriate. In our case, the basal plane consists of three

Table IV. Compositions of Atom Distribution Models for Least-Squares Refinements

	Site I	Site II			Site III		
Model	Al (At. Pct)	Al (At. Pct)	Ni (At. Pct)	Cu (At. Pct)	Al (At. Pct)	Ni (At. Pct)	Cu (At. Pct)
1	100	0.0	14.56	85.44	4.28	0.0	95.72
2	100	2.85	4.85	92.30	2.85	4.85	92.30
3	100	5.27	2.43	92.30	1.64	6.07	92.29
4	100	8.56	0.0	91.44	0.0	7.28	92.72
5	100	8.56	14.56	76.88	0.0	0.0	100
6	100	0.0	0.0	100	4.27	7.28	88.44

kinds of atoms, all different in size (Al, largest; Cu1, intermediate; Cu2, smallest). Accordingly, the smallest Cu2 atom moves toward the center of the unit cell along the *b*-axis, as indicated by arrows in Figure 3, giving the most stability. Similarly, because atom Cu2 is smaller than Cu1, the center of the triangle formed by one Cul and two Cu2 atoms will become closer to two Cu2 atoms. Therefore, atom Al in the second layer (dotted circle in Figure 3) is displaced toward two Cu2 atoms, resulting in the displacement along the *a*-axis. This movement of the largest Al will subsequently push two Cu2 atoms to the right-hand side in the first layer. Thus, the presence of atom displacements from ideal positions in Figure 3 can easily be rationalized by the rigid sphere model.

It is worthwhile to discuss the structural study in another martensitic phase, β_1'', in the Cu-Al-Ni system (β_1'' is a stress-induced martensite from the γ_1' phase, having the same basal plane as γ_1'), reported by Otsuka *et al.*[12] From four-circle neutron diffractometer measurements, they also reported similar atom displacements from ideal positions. Owing to insufficient data, however, only a rough evaluation of displacements was obtained, based on two assumptions: the basal plane is displaced as a whole (*i.e.*, every atom shifts together instead of independently) and the direction of shifting is restricted to just along the *a*-axis. Now, the present work has shown unambiguously that the displacements of atoms are present even within the basal plane.

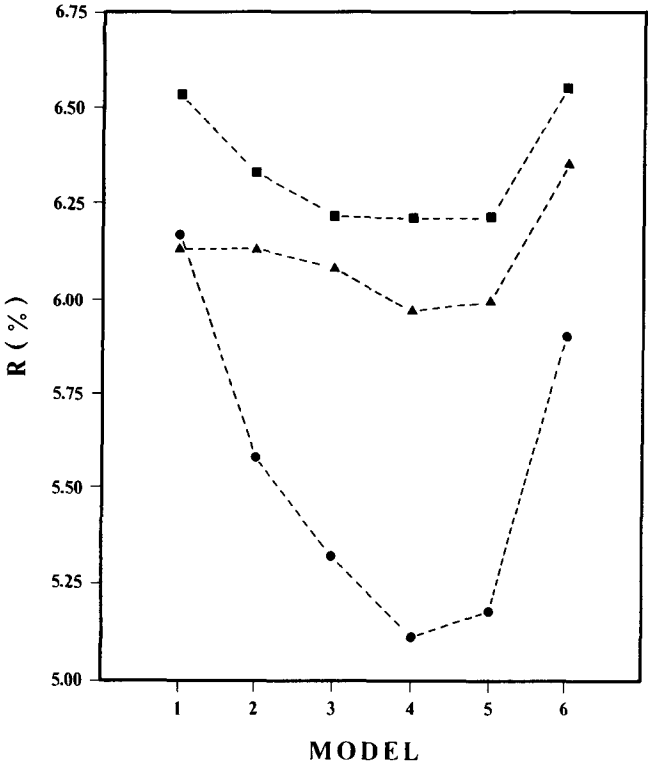

Fig. 5—*R* factor *vs* atom distribution model as a result of least-squares refinements. Abscissa: number of atom distribution model; ordinate: discrepancy factor *R*. Circles, squares, and triangles represent those of λ_1, λ_2, and λ_3, respectively.

ACKNOWLEDGMENTS

The authors wish to express their sincere appreciation to Dr. H. Horiuchi and Dr. N. Haga, University of Tokyo, and Dr. T. Ohba, University of Tsukuba, for valuable discussions. They are also grateful to Dr. S. Sasaki, KEK, and Mr. K. Morii, University of Tsukuba. Their assistance was indispensable for the present work.

REFERENCES

1. G. Kurdjumov and L.G. Khandros: *Dokl. Acad. Nauk SSSR*, 1949, vol. 66, pp. 211-16.
2. I.A. Arbuzova and L.G. Khandros: *Fiz. Met. Metalloved.*, 1964, vol. 17, pp. 390-99.
3. K. Otsuka and K. Shimizu: *Scripta Metall.*, 1970, vol. 4, pp. 469-72.
4. K. Otsuka: *Jpn. J. Appl. Phys.*, 1971, vol. 10, pp. 571-79.
5. K. Oishi and L.C. Brown: *Metall. Trans.*, 1971, vol. 2, pp. 1971-77.
6. W.A. Rachinger: *Br. J. Appl. Phys.*, 1958, vol. 9, pp. 250-52.
7. K. Otsuka, C.M. Wayman, K. Nakai, H. Sakamoto, and K. Shimizu: *Acta Metall.*, 1976, vol. 24, pp. 207-26.
8. K. Otsuka, H. Sakamoto, and K. Shimizu: *Scripta Metall.*, 1976, vol. 10, pp. 983-88.
9. V.V. Martynov and L.G. Khandros: *Dokl. Akad. Nauk SSSR*, 1977, vol. 233, pp. 345-48.
10. V.V. Martynov and L.G. Khandros: *Dokl. Akad. Nauk SSSR*, 1977, vol. 237, pp. 1349-51.
11. K. Otsuka, H. Sakamoto, and K. Shimizu: *Acta Metall.*, 1979, vol. 27, pp. 585-601.
12. K. Otsuka, M. Tokonami, K. Shimizu, Y. Iwata, and I. Shibuya: *Acta Metall.*, 1979, vol. 27, pp. 965-72.
13. M. Tokonami, K. Otsuka, K. Shimizu, Y. Iwata, and I. Shibuya: *Proc. ICOMAT-79*, MIT, Cambridge, MA, 1979, pp. 639-44.
14. K. Otsuka and K. Shimizu: *Proc. ICOMAT-79*, MIT, Cambridge, MA, 1979, pp. 607-18.
15. L.G. Khandros and V.V. Martynov: *Scripta Metall.*, 1979, vol. 13, pp. 685-88.
16. V.V. Martynov and L.G. Khandros: *Fiz. Met. Metalloved.*, 1981, vol. 51, pp. 603-08.
17. K. Otsuka and K. Shimizu: *Proc. Int. Conf. Solid-Solid Phase Transformations*, H.I. Aaronson, D.E. Laughlin, R.E. Sekerka, and C.M. Wayman, eds., 1981, pp. 1267-86.
18. H. Sakamoto, K. Shimizu, and K. Otsuka: *Trans. Jpn. Inst. Met.*, 1985, vol. 26, pp. 638-45.

19. H. Sakamoto and K. Shimizu: *Trans. Jpn. Inst. Met.*, 1987, vol. 28, pp. 715-22.
20. G. Wasserman: *Metallwirtsch.*, 1934, vol. 13, p. 133.
21. M.J. Duggin and W.A. Rachinger: *Acta Metall.*, 1964, vol. 12, pp. 529-35.
22. G. Kurdjumov, V. Mirezky, and T. Stelletzkaja: *J. Phys. Acad. Sci. USSR*, 1940, vol. 3, pp. 297-308.
23. W.G. Burgers: *Physica*, 1934, vol. 1, pp. 561-86.
24. M.J. Duggin: *Acta Metall.*, 1966, vol. 14, pp. 123-29.
25. H. Sakamoto, K. Otsuka, and K. Shimizu: *Scripta Metall.*, 1977, vol. 11, pp. 607-11.
26. H.K. Birnbaum and T.A. Read: *Trans. AIME*, 1960, vol. 218, pp. 662-69.
27. D. Schofield and A.P. Miodownik: *Met. Technol.*, April 1980, pp. 167-73.
28. G. Scarsbrook, J. Cook, and W.M. Stobbs: *J. Phys., Suppl.*, 1982, vol. 43, pp. C4-703-08.
29. N. Otani, Y. Funatsu, S. Ichinose, S. Miyazaki, and K. Otsuka: *Scripta Metall.*, 1983, vol. 17, pp. 745-50.
30. P. Coppens and W.C. Hamilton: *Acta Crystallogr.*, 1970, vol. A26, pp. 71-83.
31. Y. Abe, K. Ohsumi, T. Tagai, and M. Tokonami: Photon Factory Activity Report, National Laboratory for High Energy Physics, Tsukuba, Japan, 1982–83, pp. VI-27.
32. J.A. Ibers and W.C. Hamilton: *International Tables for X-ray Crystallography*, Kynoch Press, Birmingham, United Kingdom, 1974, vol. IV, pp. 71-98 and 148-50.
33. T. Hahn: *International Tables for Crystallography*, Kluwer Academic Publishers, Dordrecht, The Netherlands, 1983, vol. A, pp. 280-83.
34. S. Sasaki: KEK Report 83-22, *Technical Information & Library*, National Laboratory for High Energy Physics, Tsukuba, Japan, 1983, pp. 10 and 54.
35. D.T. Cromer: *J. Appl. Crystallogr.*, 1983, vol. 16, p. 437.
36. D.T. Cromer and D. Liberman: *J. Chem. Phys.*, 1970, vol. 53, pp. 1891-98.
37. T. Tadaki, M. Tokoro, and K. Shimizu: *Trans. Jpn. Inst. Met.*, 1975, vol. 16, pp. 285-96.